Robustness in TDMA Scheduling for Neuron-based Molecular Communication

Junichi Suzuki
Department of Computer Science
University of Massachusetts, Boston
Boston, MA, 02125-3393, USA
jxs@cs.umb.edu

Harry Budiman
Department of Computer Science
University of Massachusetts, Boston
Boston, MA, 02125-3393, USA
hbudiman@cs.umb.edu

ABSTRACT

This paper proposes and evaluates an optimizer for neuron-based body-area nanonetworks (BANNs). The proposed optimizer leverages an evolutionary algorithm to seek the optimal trade-off between communication latency and robustness in TDMA-based neuronal signaling. Simulation results demonstrate that the proposed optimizer efficiently obtains quality solutions and multiobjective analysis is critical in configuring neuron-based BANNs.

Categories and Subject Descriptors

C.2.2 [**Computer-Communication Networks**]: Network Protocols; C.3 [**Special-purpose and Application-based Systems**]: *Signal processing systems*; I.2.8 [**Artificial Intelligence**]: Problem Solving, Control Methods, and Search—*Heuristic methods*

General Terms

Algorithms

Keywords

Molecular communication, Neuronal networks, TDMA scheduling, Evolutionary multiobjective optimization algorithms

1. INTRODUCTION

Molecular communication is a communication paradigm that utilizes molecules as a communication medium between nanomachines. Nanomachines are nanoscale devices that perform simple computation, sensing and/or actuation tasks [18]. They may be man-made devices built in the *top-down* approach, downscaling the current microelectronic and micro-electro-mechanical technologies or in the *bottom-up* approach, assembling synthesized nanomaterials such as graphene nano ribbons and carbon nanotubes [1]. Alternatively, nanomachines may be *bio-hybrid*, integrating man-made nanostructures with biological components such as DNA strands, antibodies and molecular motors [1]. Due to its advantages such as inherent nanometer scale, biocompatibility and energy efficiency [6], a key application domain of molecular communication is body area nanonetworks (BANNs), where nanomachines are networked through molecular communication to perform their tasks in the body for biomedical and prosthetic purposes (e.g., vital information sensing, targeted drug release and neural signal augmentation) [3].

An approach to BANNs is to utilize neurons as a primary communication component [4, 19, 20]. A neuron-based BANN consists of a set of nanomachines and a network of neurons that are artificially formed into a particular topology. It allows nanomachines to interface (i.e., activate and deactivate) neurons and communicate to other nanomachines with electrochemical signals through a chain of neurons.

This paper focuses on a communication protocol framework, called Neuronal TDMA [20], which performs single-bit Time Division Multiple Access (TDMA) scheduling for neuron-based BANNs. Neuronal TDMA allows nanomachines to multiplex and parallelize neuronal signaling while avoiding signal interference to ensure that signals reach the destination. This paper proposes and evaluates a particular optimizer for Neuronal TDMA. The proposed optimizer seeks the optimal signaling schedules (i.e., which neurons to activate and when to activate them to trigger signal transmissions) for nanomachines with respect to communication latency and robustness. Communication robustness refers to the sensitivity of a signaling schedule to environmental noise that can cause signal interference.

Latency and robustness conflict with each other in neuronal signaling. For example, improving (i.e., decreasing) latency often means improving throughput in a neuronal network by increasing the degree of multiplexing. This can degrade robustness because a highly-multiplexed network has a higher risk of signal interference due to environmental noise. Conversely, improving robustness often means multiplexing neuronal signals less often. This can degrade latency because a rarely-multiplexed network tends to be low-throughput.

A goal of the proposed optimizer in Neuronal TDMA is to reveal the optimal trade-offs between communication latency and robustness subject to given constraints. Since there exists no single optimal solution (TDMA schedule) under conflicting objectives but rather a set of alternative solutions of equivalent quality, the proposed optimizer is designed to seek Pareto-optimal solutions that are distributed well in the objective space. Therefore, it can produce both *extreme* TDMA schedules (e.g., the one yielding low latency and low robustness) and *balanced* schedules (e.g., the one yielding moderate latency and robustness) at the same time.

.

Given a set of heuristically-approximated Pareto-optimal TDMA schedules, the proposed optimizer allows the BANN designer to examine the trade-offs among them and make a well-informed decision to choose one of them, as the best TDMA schedule, according to his/her preferences and priorities. For example, the BANN designer can examine how he/she can trade (or sacrifice) latency for robustness and determine a particular TDMA schedule that yields a desirable/comfortable balance between latency and robustness.

Simulation evaluation results show that the proposed optimizer in Neuronal TDMA efficiently obtains quality solutions with acceptable computational costs and verify multiobjective analysis is critical in configuring and operating neuron-based BANNs.

2. BACKGROUND

This section describes the structural and behavioral properties of neurons. Neurons are a fundamental component of the nervous system, which includes the brain and the spinal cord. They are electrically excitable cells that process and transmit information via electrical and chemical signaling.

The structure of a neuron consists of a cell body (or soma), dendrites and an axon (Figure 1). The soma is the central part of a neuron. It can vary from 4 to 100 micrometers in diameter. Dendrites are thin structures that arise from the soma. They form a complex "dendritic tree" that extends the farthest branch a few hundred micrometers from the soma. Dendrites are where the majority of inputs to a neuron occur. An axon is a cellular extension that arises from the soma. It branches before it terminates and travels through the body in bundles called nerves. Its length can be over one meter in the human nerve that arises from the spinal cord to a toe.

Neurons are connected with each other to form a network(s). Neurons communicate with others via *synapses*, each of which is a membrane-to-membrane junction between two neurons. A synapse contains molecular machinery that allows a (presynaptic) neuron to transmit a chemical signal to another (postsynaptic) neuron. In general, signals are transmitted from the axon of a presynaptic neuron to a dendrite of a presynaptic neuron. An axon transmits an output signal to a postsynaptic neuron, and a dendrite receives an input signal from a presynaptic neuron.

Presynaptic and postsynaptic neurons maintain voltage gradients across their membranes by means of voltage-gated ion channels, which are embedded in the presynaptic membrane to generate the differences between intracellular and extracellular concentration of ions (e.g., Ca^{2+}) [17]. Changes in the cross-membrane ion concentration (i.e., voltage) can alter the function of ion channels. If the concentration (i.e., voltage) changes by a large enough amount (e.g., approximately 80 mV in a giant squid), ion channels initiate a voltage-dependent process; they pump extracellular ions inward. Upon the increase in intracellular ion concentration, the presynaptic neuron releases a chemical called a *neurotransmitter* (e.g., acetylcholine (ACh)), which travels through the synapse from the presynaptic neuron's axon terminal to the postsynaptic neuron's dendrite. The neurotransmitter electrically excites the postsynaptic neuron, and the neuron generates an electrical pulse called an *action potential*. This signal travels rapidly along the neuron's axon and activates synaptic connections (i.e., opens ion channels) when it arrives at the axon's terminals. This way, an action potential

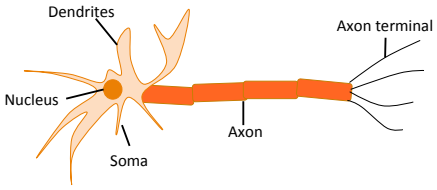

Figure 1: The structure of neurons

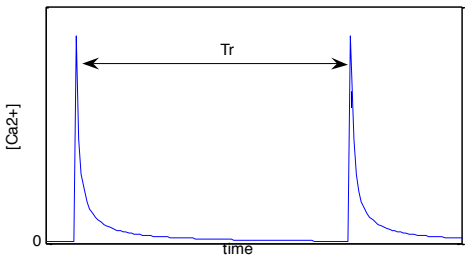

Figure 2: Intracellular Ca^{2+} concentration

triggers cascading neuron-to-neuron communication.

Figure 2 shows how Ca^{2+} concentration changes in a neuron. When the concentration peaks, the neuron releases a neurotransmitter to trigger an action potential. Upon a neurotransmitter release, the neuron goes into a *refractory period* (T_r in Figure 2), which is the time required for the neuron to replenish its internal Ca^{2+} store. During T_r, it cannot process any incoming signals. The refractory period is approximately two milliseconds in a giant squid.

3. RELATED WORK

There exist two major thrusts in communication research for body area nanonetworks (BANNs). One thrust is leveraging electromagnetic terahertz communication with, for example, graphene-based nanoscale antennas [2]. The other is molecular communication, which this paper focuses on. In general, molecular communication maintains several advantages over electromagnetic communication such as biocompatibility and energy efficiency [3, 6].

Compared with other molecular communication approaches (e.g., molecular motors [12], calcium signaling [14] and bacteria communication [10]), neuron-based communication has such advantages as long distance coverage, high speed signaling (up to 90 m/s [8]) and low attenuation in signaling [6].

Balasubramaniam et al. first examined TDMA communication for neuronal signaling [4]. Neuronal TDMA extended it with a multiobjective optimization algorithm that considers communication performance objectives such as signaling yield, fairness and latency [20]. This paper extends Neuronal TDMA by analyzing the optimal trade-offs between communication performance (latency) and robustness.

Tezcan et al. address communication robustness in TDMA-based neural signaling by proposing a signal buffering mechanism with neural delay lines, which parallel fiber delay lines in optical network switching. The proposed optimizer in this paper is similar to their mechanism in that both aim to avoid signal interference. However, this paper addresses robustness in the context of optimizing TDMA schedules while Tezcan et al. do not consider TDMA scheduling.

4. NEURON-BASED BODY AREA NANONETWORKS (BANNS)

This paper assumes neural signaling in a network of natural neurons that are artificially grown and formed into particular topology patterns. This assumption is made upon numerous research efforts to grow neurons on substrates (e.g., [15]) and design topologically-specific neuronal networks (e.g., [9, 13, 21]).

Figure 3 illustrates an example neuron-based BANN. It contains an artificially-grown neuronal network and several nanomachines such as sensors and a sink. Sensors use neuronal signaling to transmit sensor data to the sink, which might work as an actuator or transducer. As potential applications, prosthetic devices and medical rehabilitation devices could leverage neuron-based BANNs to better perform sensing, transducing and actuation tasks in the body.

This paper assumes that nanomachines (e.g., sensors) interact with neuronal networks in a *non-invasive* manner. This means that it is not required to insert carbon nanotubes into neurons so that nanomachines can trigger signaling. Nanomachines may use a neurointerface based on chemical agents (e.g., acetylcholine and mecamylamine [4]) or light [7].

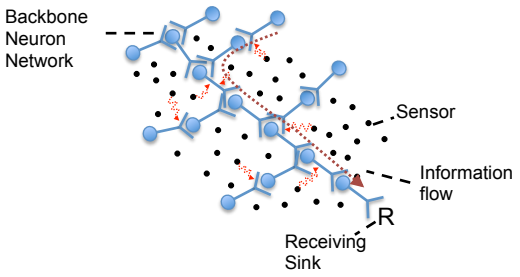

Figure 3: An Example Neuron-based BANN

5. NEURONAL TDMA

Neuronal TDMA performs a single-bit TDMA communication that periodically assigns a *time slot* to each sensor. Sensors fire neurons, one after the other, each using its own time slot. This allows multiple sensors to transmit signals to the sink through the shared neuronal network. Each sensor transmits a single signal (a single bit) within a single time slot. This single-bit-per-slot design is based on two assumptions: (1) a signal (i.e., action potential) is interpreted with two levels of amplitudes, which represent 0 and 1, and (2) after a signal transmission, a neuron goes into a refractory period (waiting/sleeping period).

An important goal of Neuronal TDMA is to avoid signal interference, which occurs when multiple signals fire the same neuron at the same time and leads to corruption of transmitted sensor data at the sink. Signals can easily interfere with each other if sensors fire their neighboring neurons randomly. Neuronal TDMA is intended to eliminate signal interference by scheduling which sensors fire which neurons with respect to time. An optimizer in Neuronal TDMA seeks the optimal TDMA schedules for a set of sensors in a given neuronal network.

Figure 4 shows an example body area nanonetwork (BANN) that contains four nanomachines (three sensors and a sink) and a network of five neurons (n_1 to n_5). Figure 5 illustrates an example TDMA schedule for those sensors to fire neurons. The scheduling cycle period lasts 6 time slots ($T_s = 5$). The sensor s_1 fires the neuron n_4 to initiate signaling in the first time slot T_1. The signal travels through n_5 in the next time slot T_2 to reach the sink. The sensor s_2 transmits a signal on n_3 in T_2. During T_2, two signals travel in the neuronal network in parallel. The duration of each time slot must be equal to, or longer than, the refractory period T_r (Figure 2).

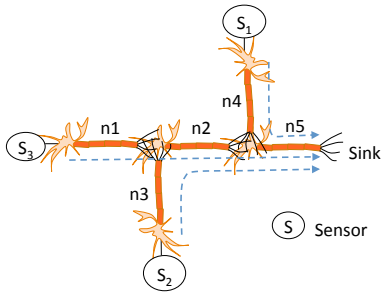

Figure 4: An Example Neuron-based BANN

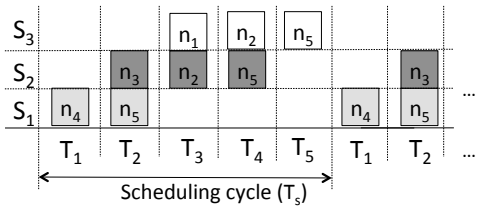

Figure 5: An Example TDMA Schedule

5.1 Scheduling Problem in Neuronal TDMA

The scheduling problem in Neuronal TDMA is defined as an optimization problem where a neuron-based BANN contains M sensors, $S = \{s_1, s_2, ..., s_i, ..., s_M\}$, and N neurons, $N = \{n_1, n_2, ..., n_j, ..., n_N\}$.

The proposed optimizer considers two optimization constraints. The first constraint enforces that at most one signal can pass through each neuron in a single time slot. (Otherwise, signal interference occurs.) The second constraint enforces each sensor transmits one signal during the scheduling cycle T_s. A TDMA schedule is said to be feasible if it never violates constraints. On the contrary, it is said to be infeasible if it violates any of these two constraints. An example TDMA schedule in Figure 5 is feasible.

The proposed optimizer considers two optimization objectives: (1) communication latency and (2) communication robustness. Latency and robustness are to be minimized and maximized, respectively.

Communication latency (f_L) indicates how soon the sink receives all signals from all of M sensors. It is computed as follows.

$$f_L = max_{s_i \in S}\ t_a^{s_i} \quad (1)$$

$t_a^{s_i}$ denotes the arrival time at which the sink receives a signal that s_i transmits. f_L determines the scheduling cycle period T_s ($T_s = f_L$). In Figure 5, $f_L = 5$.

Communication robustness (f_R) indicates the probability that signals do not interfere with each other on shared neurons $N^{'} = \{n_1^{'}, n_2^{'}, ..., n_k^{'}, ..., n_K^{'}\} \in N$. Shared neurons are the neurons that sensors share to transmit their signals to the sink. In Figure 5, n_2 and n_5 are shared neurons. (s_2

and s_3 share n_2. s_1, s_2 and s_3 share n_5.) Higher robustness means lower chances of signal interference that can occur due to variances of signal transmission speed in a neuron even if the *one-signal-per-slot* constraint (see above) is satisfied. In Figure 5, s_2's signal travels on n_2 in T_3, and s_3's signal travels on n_2 in T_4. This signaling schedule satisfies the *one-signal-per-slot* constraint; however, the two signals can interfere if s_2's signal arrives at n_2 during T_4 due to variances signal transmission speed in n_2 and/or if s_3's signal arrives at n_2 in T_3 due to signaling speed variances in n_1.

A major contributor to the variances of signal transmission speed is *synaptic delay*, which is the interval between the arrival of an action potential at a presynaptic axon terminal and the start of a postsynaptic action potential. This interval is the time required for a neurotransmitter to be released from a presynaptic membrane, diffuse across the synaptic gap and bind to a receptor site on the post-synaptic membrane. It is known that a synaptic delay varies from $0.3-0.5$ milliseconds to several milliseconds.

Figure 6 shows a statistical model to determine the probability of signal interference. Figure 6(a) shows two signals from s_1 and s_2 and their expected arrival times at $n_k^{'}$ ($t_{s_i}^{n_k}$ and $t_{s_j}^{n_k}$). T represents the interval between the two arrival times. Arrival times follow a normal distribution with a standard deviation of σ. Figure 6(b) depicts $N(t_{s_i}^{n_k^{'}}, \sigma^2) - N(t_{s_j}^{n_k^{'}}, \sigma^2)$, which illustrates the probability that two distributions ($N(t_{s_i}^{n_k^{'}}, \sigma^2)$ and $N(t_{s_j}^{n_k^{'}})$) overlap. F is the cumulative distribution function for $N(t_{s_i}^{n_k^{'}}, \sigma^2) - N(t_{s_j}^{n_k^{'}}, \sigma^2)$. $F(0)_{s_i,s_j}^{n_k^{'}}$ denotes the probability that two signals from s_1 and s_2 do not interfere.

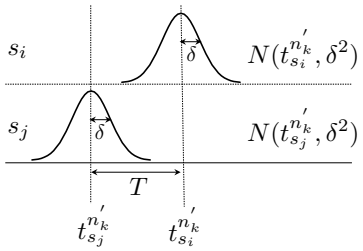

(a) Variances of the Arrival Times of Two Signals from Sensors s_i and s_j

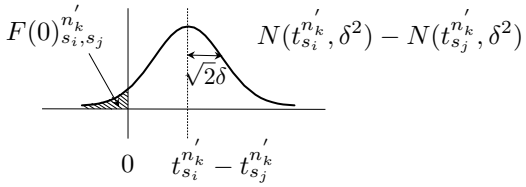

(b) Probability of Signal Interference on a Shared Neuron $n_k^{'}$ between Sensors s_i and s_j

Figure 6: Robustness in Neural Signaling

The communication robustness objective (f_R) is computed as follows by generalizing the model described in Figure 6.

$$f_R = -\sum_{i=1}^{M}\sum_{j=1}^{M}\sum_{k=1}^{K}\left(F(0)_{s_i,s_j}^{n_k^{'}} \times I_s\right)$$
$$\text{where } F(0)_{s_i,s_j}^{n_k^{'}} = \frac{1}{2}\left(1 + \frac{1}{\sqrt{\pi}}\int_{-\frac{T}{2\sigma}}^{\frac{T}{2\sigma}} e^{-x^2}\,\mathrm{d}x\right) \quad (2)$$

Note that $I_s = 1$ if $t_{s_i}^{n_k} > t_{s_j}^{n_k}$; otherwise, $I_s = 0$.

5.2 The Proposed Optimizer in Neuronal TDMA

The proposed optimizer in Neuronal TDMA leverages an evolutionary multiobjective optimization algorithm (EMOA) to solve its scheduling optimization problem. The algorithm iteratively evolves the population of solution candidates, called *individuals*, through several operators (e.g., crossover, mutation and selection operators) toward the Pareto-optimal solutions in the objective space.

In order to seek Pareto optimality, the notion of *dominance* plays an important role [16]. An individual i is said to dominate an individual j if both of the following conditions are hold.

- i's objective values are superior than, or equal to, j's in all objectives.
- i's objective values are superior than j's in at least one objectives.

In Neuronal TDMA, each individual represents a particular TDMA schedule for M sensors. Figure 7 shows the structure of an example individual, which represents the schedule shown in Figure 5. In this example, the first sensor, s_1, fires its neighboring neuron, n_4, in the first time slot T_1. Similarly, $s2$ and s_3 fire their neighboring neurons (n_2 and n_1) in T_2 and T_3, respectively.

S_3	0	0	1	0	0
S_2	0	1	0	0	0
S_1	1	0	0	0	0
	T_1	T_2	T_3	T_4	T_5

Figure 7: Individual Representation

Algorithm 1 shows how the proposed optimizer works. It follows the algorithmic structure in NSGA-II [5]. At the 0-th generation, N individuals are randomly generated as the initial population $\mathcal{P}_0$ (Line 2).

In each generation (g), two parent individuals (p_1 and p_2) are selected from the current population $\mathcal{P}_g$ with binary tournaments (Lines 6 and 7). A binary tournament randomly takes two individuals from $\mathcal{P}_g$, compares them based on the notion of dominance, and chooses a superior one as a parent. With the crossover rate P_c, two parents reproduce two offspring through crossover (Lines 8 to 10). Then, mutation occurs on each offspring (Lines 11 to 16). It randomly alters a neuron-firing pattern with the mutation rate P_m. The binary tournament, crossover and mutation operators are executed repeatedly on $\mathcal{P}_g$ to reproduce N offspring. The offspring ($\mathcal{O}_g$) are combined with the parent population $\mathcal{P}_g$ to form $\mathcal{R}_g$ (Line 19).

Algorithm 1 Optimization Process

```
1: g = 0;
2: P_g = Randomly generated N individuals;
3: while g < G_max do
4:    O_g = ∅;
5:    while |O_g| < N do
6:       p_1 = tournament(P_g)
7:       p_2 = tournament(P_g)
8:       if random() ≤ P_c then
9:          {o_1, o_2} = crossover(p_1, p_2)
10:      end if
11:      if (random() ≤ P_m) then
12:         o_1 = mutation(o_1)
13:      end if
14:      if random() ≤ P_m then
15:         o_2 = mutation(o_2)
16:      end if
17:      O_g = {o_1, o_2} ∪ O_g
18:   end while
19:   R_g = P_g ∪ O_g
20:   F = sortByDominationRanking(R_g)
21:   P_{g+1} = {∅}
22:   i = 1
23:   while |P_{g+1}| + |F_i| ≤ N do
24:      P_{g+1} = P_{g+1} ∪ F_i
25:      i = i + 1
26:   end while
27:   sortByCrowdingDistance(F_i)
28:   P_{g+1} = P_{g+1} ∪ F_i[1 : (N − |P_{g+1}|)]
29:   g = g + 1
30: end while
```

Environmental selection follows reproduction. Best N individuals are selected from $2N$ individuals in $\mathcal{R}_g$ as the next generation population ($\mathcal{P}_{g+1}$). First, the individuals in $\mathcal{R}_g$ are ranked based on the dominance relationships among them. Non-dominated individuals are on the first rank. The i-th rank consists of the individuals dominated only by the individuals on the $(i-1)$-th rank. Ranked individuals are stored in $\mathcal{F}$ (Line 20). $\mathcal{F}_i$ contains the i-th rank individuals.

Then, the individuals in $\mathcal{F}$ move to $\mathcal{P}_{g+1}$ on a rank by rank basis, starting with $\mathcal{F}_1$ (Lines 23 to 26). If the number of individuals in $\mathcal{P}_{g+1} \cup \mathcal{F}_i$ is less than N, $\mathcal{F}_i$ moves to $\mathcal{P}_{g+1}$. Otherwise, a subset of $\mathcal{F}_i$ moves to $\mathcal{P}_{g+1}$. The subset is selected based on the crowding distance metric, which measures the distribution (or diversity) of individuals in the objective space [5] (Lines 27 and 28). The metric computes the distance between two closest neighbors of an individual in each objective and sums up the distances associated with all objectives. A higher crowding distance means that an individual in question is more distant from its neighboring individuals in the objective space. In Line 27, the individuals in $\mathcal{F}_i$ are sorted from the one with the highest crowding distance to the one with the lowest crowding distance. The individuals with higher crowding distance measures have higher chances to be selected to $\mathcal{P}_{g+1}$ (Line 28).

6. EVALUATION

This section evaluates the proposed optimizer in Neuronal TDMA through simulations.

6.1 Simulation Configurations

This paper simulates a neuronal network that contains 43 neurons (Figures 8). 11 sensors are evenly distributed in the network. The network topology is generated with a tree structure generation algorithm based on Diffusion Limited Aggregation (DLA) [11].

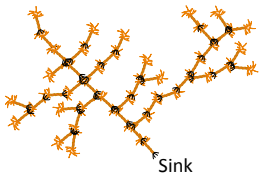

Figure 8: A Simulated Neuronal Network

The proposed optimizer is configured with a set of parameters shown in Table 1. Q denotes the total number of time slots in an individual ($Q = 15$ in Figure 7). T_u denotes the amount of time allocated to each time slot.

Table 1: EMOA Configurations

Parameter	Value
Max. # of generations (g_{max} in Figure 1)	100
Population size (N in Figure 1)	100
Crossover rate (P_c in Figure 1)	0.9
Mutation rate (P_m in Figure 1)	$1/Q$
σ in Equation 2	$T_u/3$

6.2 Simulation Results

Figure 9(a) shows how the proposed optimizer increases the union of the hypervolumes (HVs) that individuals dominate in the objective space as the number of generations grows. The HV metric quantifies the optimality and diversity of individuals [22]. A higher HV means that individuals are closer to the Pareto-optimal front and more diverse in the objective space. As Figure 9(a) shows, the proposed optimizer rapidly increases its HV measure in the first 20 generations and converges around the 60th generation. At the last generation, all individuals are non-dominated in the population. This demonstrates that the proposed optimizer allows individuals to efficiently evolve and improve their quality and diversity within 100 generation.

Figure 9(b) shows an objective space that plots the individuals obtained at the last generation. Those individuals approximate the Pareto front (i.e., the optimal tradeoff) between latency and robustness. Note that the robustness of -20% means the signal interference probability of 20%. Given objective value ranges ($16 \leq T_L \leq 47$ and $-40.77 \leq T_R \lessapprox 0$), the BANN designer can examine how he/she can trade latency for robustness and choose a particular individual as the best TDMA schedule according to his/her preferences, priorities and/or constraints.

7. CONCLUSIONS

The proposed optimizer in Neuronal TDMA is designed to optimize TDMA signaling schedules for nanomachines in neuron-based BANNs. Simulation results demonstrate that the proposed optimizer efficiently obtains quality solutions and multiobjective analysis is critical in configuring neuron-based BANNs.

8. REFERENCES

[1] I. Akyildiz, F. Brunetti, and C. Blazquez. Nanonetworks: a new communication paradigm. *Computer Networks Journal*, 52(12), 2008.

[2] I. Akyildiz and J. M. Jornet. Electromagnetic wireless nanosensor networks. *Elsevier Nano Communication Networks*, 1(1), 2010.

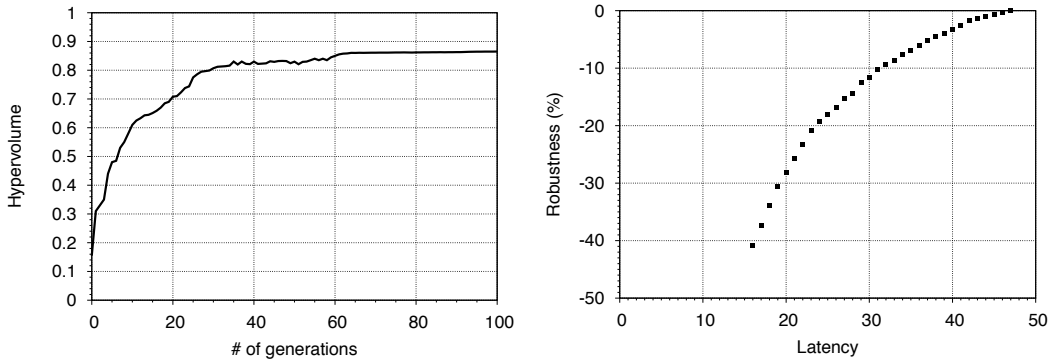

(a) Hypervolume (b) Trade-off between Latency and Robustness

Figure 9: Simulation Results

[3] B. Atakan, S. Balasubramaniam, and O. B. Akan. Body area nanonetworks with molecular communications in nanomedicine. *IEEE Communications Magazine*, January 2012.

[4] S. Balasubramaniam, N. T. Boyle, A. Della-Chiesa, F. Walsh, A. Mardinoglu, D. Botvich, and A. Prina-Mello. Development of artificial neuronal networks for molecular communication. *Nano Communication Networks*, 2(2-3), 2011.

[5] K. Deb, S. Agrawal, A. Pratab, and T. Meyarivan. A fast elitist non-dominated sorting genetic algorithm for multi-objective optimization: NSGA-II. In *Proc. Conf. Parallel Problem Solving from Nature*, 2000.

[6] L. P. Gine and I. F. Akyildiz. Molecular communication options for long range nanonetworks. *Computer Networks*, 53, 2009.

[7] N. Grossman, K. Nikolic, and P. Degenaar. The neurophotonic interface: stimulating neurons with light. *The Neuromorphic Engineer*, 2008.

[8] J. B. Hursh. Conduction velocity and diameter of nerve fibers. *Amer. J. Physiol.*, 127, 1939.

[9] S. B. Jun, M. R. Hynd, N. Dowell-Mesfin, K. L. Smith, J. N. Turner, W. Shain, and S. J. Kima. Low-density neuronal networks cultured using patterned polyl-L-lysine on microelectrode arrays. *Journal of Neurosci. Methods*, 160(2), 2007.

[10] P. Lio and S. Balasubramaniam. Opportunistic routing through conjugation in bacteria communication nanonetwork. *Nano Comm. Networks*, 3(1), 2012.

[11] A. Luczak. Measuring neuronal branching patterns using model-based approach. *Front. Comput. Neurosci.*, 4(135), 2010.

[12] M. Moore, A. Enomoto, T. Nakano, R. Egashira, T. Suda, A. Kayasuga, H. Kojima, H. Sakakibara, and K. Oiwa. A design of a molecular communication system for nanomachines using molecular motors. In *Proc. IEEE Int'l Conference on Pervasive Computing and Communications Workshops*, 2006.

[13] F. Morin, N. Nishimura, L. Griscomb, B. LePioufle, H. Fujita, Y. Takamura, and E. Tamiya. Constraining the connectivity of neuronal networks cultured on microelectrode arrays with microSSuidic techniques: A step towards neuron-based functional chips. *Biosensors and Bioelectronics*, 21, 2006.

[14] T. Nakano, T. Suda, M. Moore, R. Egashira, A. Enomoto, and K. Arima. Molecular communication for nanomachines using intercellular calcium signaling. In *Proc. IEEE Int'l Conf. on Nanotechnology*, 2005.

[15] T. D. Nguyen-Vu, H. Chen, A. M. Cassell, R. J. Andrews, M. Meyyappan, and J. Li. Vertically aligned carbon nanofiber architecture as a multifunctional 3-D neural electrical interface. *IEEE Trans. Biomed. Eng.*, 54(6), 2007.

[16] N. Srinivas and K. Deb. Multiobjective function optimization using nondominated sorting genetic algorithms. *Evol. Computat.*, 2(3), 1995.

[17] G. Stuart, J. Schiller, and B. Sakmann. Action potential initiation and propagation in rat neocortical pyramidal neurons. *Journal of Physiology*, 505.3, 1997.

[18] T. Suda, M. Moore, T. Nakano, R. Egashira, and A. Enomoto. Exploratory research on molecular communication between nanomachines. In *Proc. ACM Genetic and Evol. Computat. Conference*, 2005.

[19] J. Suzuki and S. Balasubramaniam. Networking and scheduling in neuron-based molecular communication. In *Proc. of NSF Workshop on Biological Computations and Communications*. November 2012.

[20] J. Suzuki, S. Balasubramaniam, and A. Prina-Mello. Multiobjective TDMA optimization for neuron-based molecular communication. In *Proc. of the 7th Int'l Conference on Body Area Networks*. September 2012.

[21] C. Wyart, C. Ybert, L. Bourdieu, C. Herr, C. Prinz, and D. Chatenay. Constrained synaptic connectivity in functional mammalian neuronal networks grown on patterned surfaces. *J. Neurosci. Methods*, 117(2), 2002.

[22] E. Zitzler and L. Thiele. Multiobjective optimization using evolutionary algorithms: A comparative study. In *Proc. Int'l Conf. on Parallel Problem Solving from Nature*, 1998.